AI Med

AI PRESS
Open Access Academic Publisher

Article

Analysis of hub genes and signalling pathways in lipomas by integrated bioinformatics

Fei Wang[1], Yuyang Xia[2], Yuxin Jia[3], Zhuyuan Zhang[4], Yu Deng[5], YuJing Wu[6], Yating Zhang[7,*]

1 Shanghai Medical College, Fudan University, Shanghai, China

2 Institute of Medicine, Sechenov First Moscow State Medical University, Moscow, Russian Federation

3 Brown School, Washington University in St.Louis, MO, USA

4 College of Basic Medical Sciences, Hebei Medical University, Shijiazhuang, China

5 Cardiology Department, Sanyuan County Traditional Chinese Medicine Hospital, Xianyang, Shanxi, China

6 School of Clinical Medicine, Jining Medical University, Jining, China

7 College of Information Engineering, Wuhan University of Technology, Wuhan, China

*Corresponding authors:
Yating zhang, zytzyt7701@163.com;

Received: 5 June 2025
Revised: 16 July 2025
Accepted: 1 Aug 2025
Published: 2 Aug 2025

© 2025 The Author(s). *AI Med* published by AI Press. This is an open access publication under the Creative Commons Attribution 4.0 International License (CC BY).

Abstract

Background: Lipomas are the most common benign tumours, but some deep lipomas are technically difficult to remove surgically. Early diagnosis and treatment of lipomas can be facilitated by early genetic biomarkers; however, the key genes and signalling pathways that influence lipoma development are not well understood. The aim of this study was to identify hub genes and signalling pathways associated with the development of lipomas.

Methods: A dataset of human lipomas (GSE141027) was first downloaded from Gene Expression Omnibus, differential genes (DEGs) for expression profiles were analysed in R software via the edgeR package, and a protein–protein interaction network was constructed. Based on preliminary data, further modular analysis, neighbour node analysis and Hubba analysis were performed using Cystoscope to identify intersecting genes and display them in a Venn diagram to obtain key hub genes. Enrichment analysis was then carried out using the ClueGO plugin in Cytoscape (v3.9). In addition, weighted gene coexpression network analysis (WGCNA) was used to identify coexpression modules positively and negatively associated with the clinicopathological features of lipoma in the whole dataset, and enrichment analysis was performed on the module genes to obtain the signalling pathways associated with the clinicopathological features of lipoma by intersecting with the signalling pathway enrichment of DEGs. All data were then used for GSEA enrichment to further validate the signalling pathways related to the clinicopathological features of lipoma.

Results: A total of 418 DEGs were identified, of which 176 were upregulated and 242 downregulated. Seventeen hub genes were identified by MCODE and hubba plug-in and collateral node analysis, including CKM, ATP2A1, MYLPF, TNNI2, MYL1, ACTN3, ACTN2, ACTG2, MYH11, NEB, MYBPC2, MYOZ1, MYH2, MYBPC1, TNNC2, ACTA1 and TCAP. TCAP. The enrichment functions and signalling pathways of the DEGs were subsequently analysed by the ClueGO plugin. A Venn diagram revealed the 15 most clinically relevant modular gene-enriched signalling pathways for lipoma (including the calcium signalling pathway and ECM-receptor interaction). In addition, 9 key signalling pathways associated with lipoma were identified using GSEA.

Conclusion: This study analysed hub genes and signalling pathways of lipoma by bioinformatics to provide potential targets and

signalling pathways for early diagnosis and treatment.

Keywords: Bioinformatics, Oncology, lipoma, WGCNA, Hub gene, Signalling pathw

Introduction

Lipomas are benign lesions of fatty tissue that affect soft tissues, including the musculoskeletal system(1). are formed by accumulation of fat, which can accumulate in many parts of the body (2). When formed in superficial areas of the body, they form one or more hard-fitting masses, which can cause fat gain and a distorted appearance(3). However, when a lipoma forms inside the body, intraosseous lipomas, in particular, are difficult to remove and can cause all kinds of damage (4). For example, nerve compression in the spine (5), neuropathy (6) and even ossification (7) in the bone can cause further damage to the body. There is an increasing number of reported cases of lipoma, hub genes and signaling pathways play an important role in the development and progression of diseases, but the molecular mechanisms of lipoma formation are still very poorly understood.

Gene Expression Omnibus (GEO) (8) is the most commonly used public database, containing a large amount of sequencing data for various disease phenotypes (9). Bioinformatics (10) is used for gene expression profiling to further investigate the molecular mechanisms and signalling pathways of disease through differential gene (DEG) (11) screening (12). An important approach to understanding the association of genes with clinicopathological features from genome-wide expression is weighted gene coexpression network analysis (WGCNA) (13). WGCNA can be used to detect coexpression modules of highly relevant genes and modules of interest associated with clinical features (14), providing insights into predicting the function of coexpressed genes and finding genes that play a key role in human disease(15). The conventional methods of bioinformatics and WGCNA are now widely used to predict the molecular mechanisms of various diseases (16, 17), and their combination can lead to the identification of more critical and reliable genes (18) and signalling pathways (19) that lead to disease development.

In this study, we first screened for DEGs in lipomas by the edgeR package (20). Hub genes were identified using three key gene analysis methods. GO and KEGG enrichment analyses were performed to identify enriched functional and signalling pathways related to the DEGs, WGNCA was used to identify modules associated with lipoma, the genes within the modules were subjected to GO and KEGG enrichment analyses to identify signalling pathways associated with lipoma, and finally, GSEA was used to validate and provide new insights into the molecular mechanisms of lipoma.

Materials and Methods

Data collection

The GEO database was searched using the keyword "lipoma", and the GSE141027 microarray dataset was downloaded. The dataset contains 30 samples: 15 samples of lipoma and 15 samples of normal adipose tissue in the vicinity of the lipoma, Organism: Homo sapiens.

Identification of DEGs

For GSE141027, all individual samples were first combined into one expression file and then corrected using the "edgeR" package. Significantly different genes were screened using $|\log2 (\text{Fold Change})| \geq 1$, $p < 0.05$.

Identification of hub genes

First, we selected "Multiple protein" on the STRING (21) website, uploaded the DEG information to the website, selected "Homo sapiens" for analysis, generated a PPI network and visualized it with the Cytoscape tool. Finally, the cytoHubba plug-in identified the central genes, the MCODE(22) plug-in analysed the important module genes, and the neighbouring nodes identified the top 20 genes with the most nodes.

DEG enrichment analysis

The Cytoscape (v3.9.0) cluego(23) plugin was used to annotate and map Gene Ontology (GO) terms, including biological processes, cellular components and molecular functions, and the Kyoto Protocol Encyclopedia of Genes and Genomes (KEGG) pathways. The enriched genes were considered DEGs.

Identifying the most relevant coexpression modules using WGCNA

A coexpression network was constructed for the 30 samples using the WGCNA package, and the samples were divided into two groups according to clinicopathological characteristics: normal adipose tissue and lipoma tissue. First, the adjacency matrix was calculated according to the optimal soft threshold, and then the adjacency matrix was converted to a topological overlap matrix (TOM) to construct a clustering dendrogram for the 30 samples. Second, the correlation coefficients between the modules and the two groups of samples were analysed, and the module with the highest positive correlation and the highest negative correlation coefficient was selected as the most relevant module for lipoma.

Module gene enrichment analysis

The modular genes with the highest positive and negative correlation coefficients from the above analysis were enriched

using *the cluego plugin, including GO and KEGG enrichment analyses.*

GSEA enrichment validation

The 30 samples were divided into normal adipose and lipoma groups, and the biological pathways of the samples were analysed by GSEA. GO genes were available from Molecular Signature Database (MsigDB) in Bioprocess Database (c5.go.bp.v7.4). NES (normalized enrichment score) was used to compare the results of the whole-genome analysis. Validation of the signalling pathways found in the previous step in relation to the clinical features of lipomas and graphical presentation of the validation results was performed.

Results

Identification of DEGs

To obtain DEGs associated with lipoma in GSE141027, we performed differential analysis using the "edgeR" package and obtained a total of 418 DEGs, which were displayed using a volcano plot (Figure 1A). The top 50 genes with the largest log2 (FC) values are displayed in a heatmap (Figure 1B). The protein interactions network (Figure S1) was used to show the protein relationships of the DEGs, and the upregulated genes (176) and downregulated genes (242) were displayed using a PPI network (Figure S2).

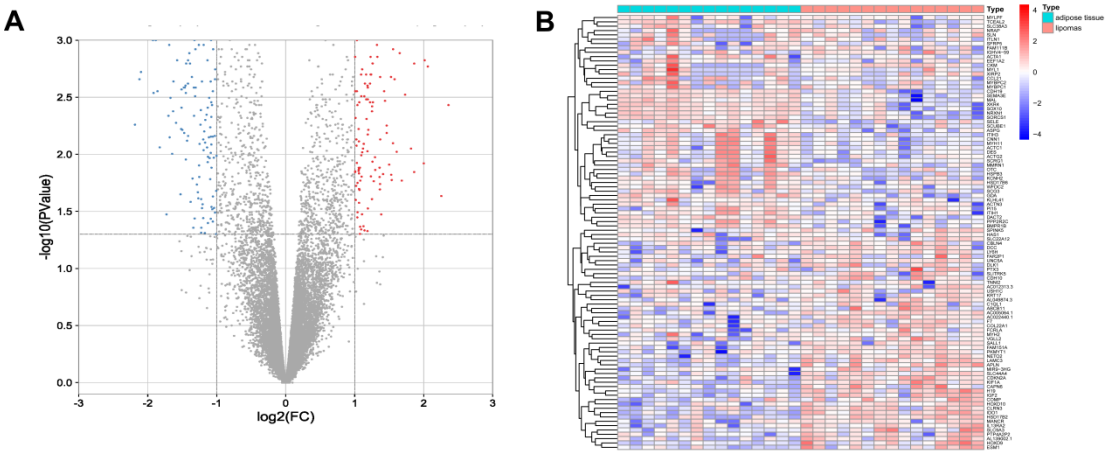


Figure 1. Identification of DEGs in the GSE141027 dataset with cut-off criteria of |log2 FC| ⩾ 1 and P < 0.05. (A) Volcano plot of DEGs in the dataset. (B) Heatmap of the top 50 DEGs in the dataset.

Identification of hub genes

To identify hub genes among the DEGs, important modules were first identified using the MCODE plugin (Figure 2A-E). Then, the number of nodes between all genes was counted using the neighbouring nodes, and the top 20 genes were selected for display (Figure 2F). Then, the Hubba plug-in was used to find the central gene of the network, and the central gene was created as a separate network (Figure 2G). The key genes found by the three methods were intersected to obtain the hub genes, which are displayed in a Venn diagram (Figure 2H).

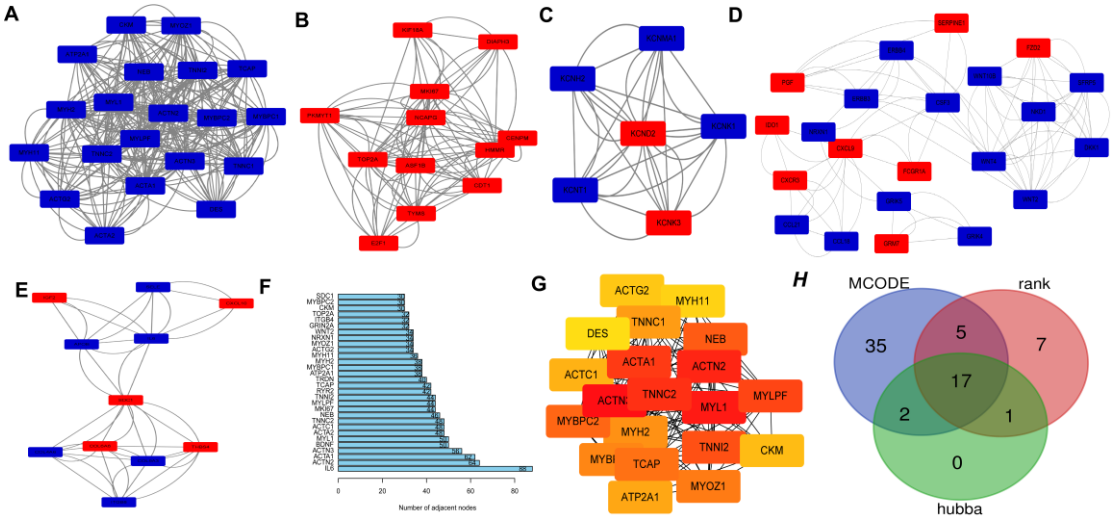


Figure 2. Hub gene identification. (A-E) Key modules found by the MCODE plugin with a composite score greater than 3. (F) Key node genes found by the collar node algorithm. (G) Key central genes found by the Hubba plugin. (F) Key genes found by the three methods taken from the intersection Venn diagram.

DEG enrichment analysis

To determine the function and signalling pathway of DEG enrichment. The Cluego plug-in was used for GO and KEGG enrichment analyses of DEGs. BP (biological process) (Figure 3A) enrichment included negative regulation of sequestering of calcium. CC (cellular component) (Figure 3B) enrichment included the basement membrane and intrinsic component of the synaptic membrane. MF (molecular function) (Figure 3C) enrichment included calcium channel The enrichment of complex and potassium channel complex. KEGG (Kyoto Encyclopedia of Genes and Genomes) (Figure 3D) pathways included the calcium signalling pathway and genome ferroptosis.

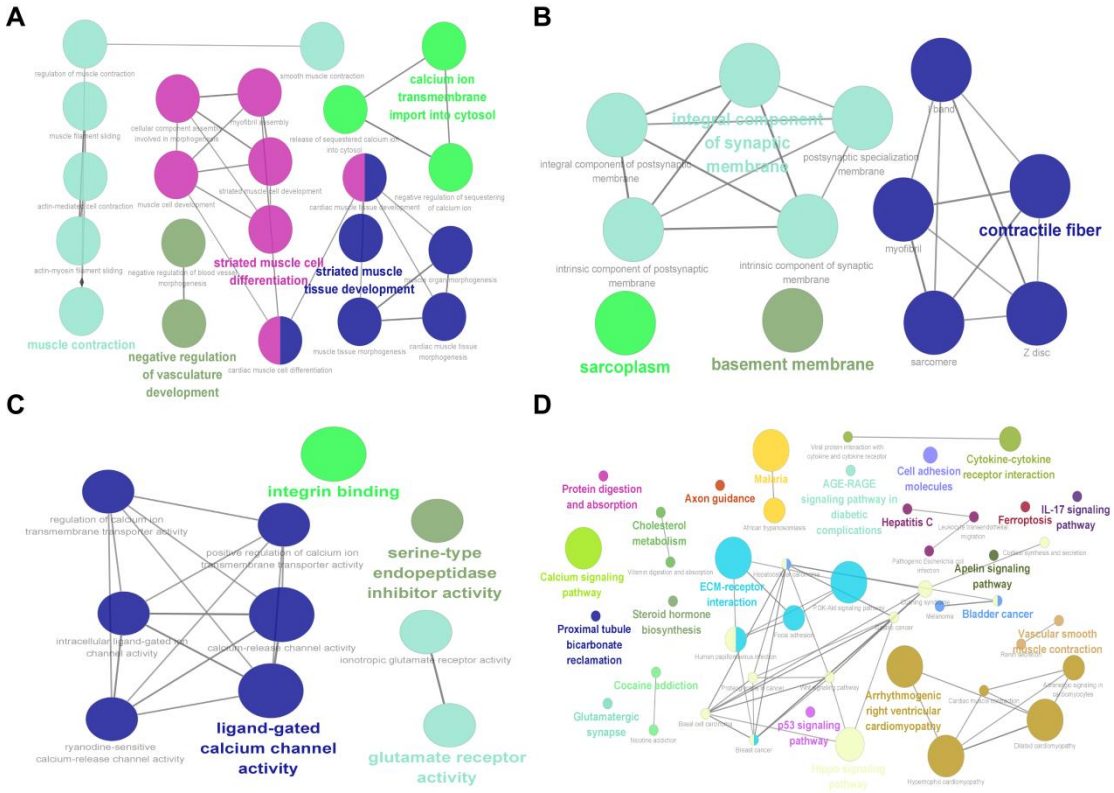


Figure 3. Results of DEG enrichment analysis. (A) Display diagram of BP. (B) Display diagram of CC. (C) Display diagram of MF. (D) Display diagram of KEGG. The colour represents the P value, and the size of the circle represents the number of genes. BP, biological process; CC, cellular component; MF, molecular function; KEGG, Kyoto Encyclopedia of Genes and Genomes.

WGCNA lipoma correlation analysis

To identify key module genes associated with lipomas, coexpression network modules associated with lipomas were constructed from the GSE141027 dataset using the WGCNA package. A clustering dendrogram of the coexpression network was first obtained (Figure 4A). The results of the module-trait relationships (Figure 4B) revealed that the royal blue module (r = 0.66, p = 8e-05) had the highest positive correlation with lipoma, and the green module (r = 0.6, p = 5e-04) had the highest negative correlation coefficient.

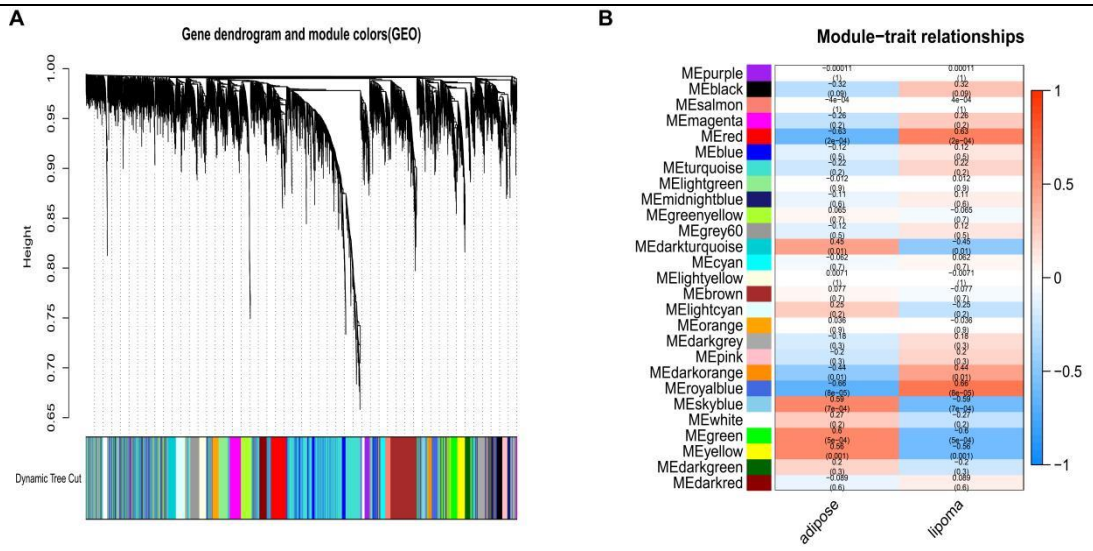


Figure 4. Identification of modules associated with clinical information on lipomas in the GSE141027 dataset. (A) Clustered dendrograms of coexpression network modules are sorted by gene hierarchical clustering based on a 1-TOM matrix. Each module is assigned a different colour. (B) Module-feature relationships. Each row corresponds to a colour module, and each column corresponds to a clinical feature (normal adipose tissue and lipoma). Each cell contains the corresponding correlation and p value.

Module gene enrichment analysis

We further identified signalling pathways associated with lipomas. BP (Figure 5A) was enriched for negative regulation of the G protein-coupled receptor signalling pathway. CC (Figure 5B) was enriched for the basal plasma membrane and extracellular matrix. MF (Figure 5C) was enriched for lipid kinase activity and bioactive lipid receptor activity. KEGG (Figure 5D) pathway enrichment included the calcium signalling pathway and mineral absorption. Subsequent intersection with the DEGs enriched signalling pathways yielded 15 (Figure E) pathways associated with lipoma.

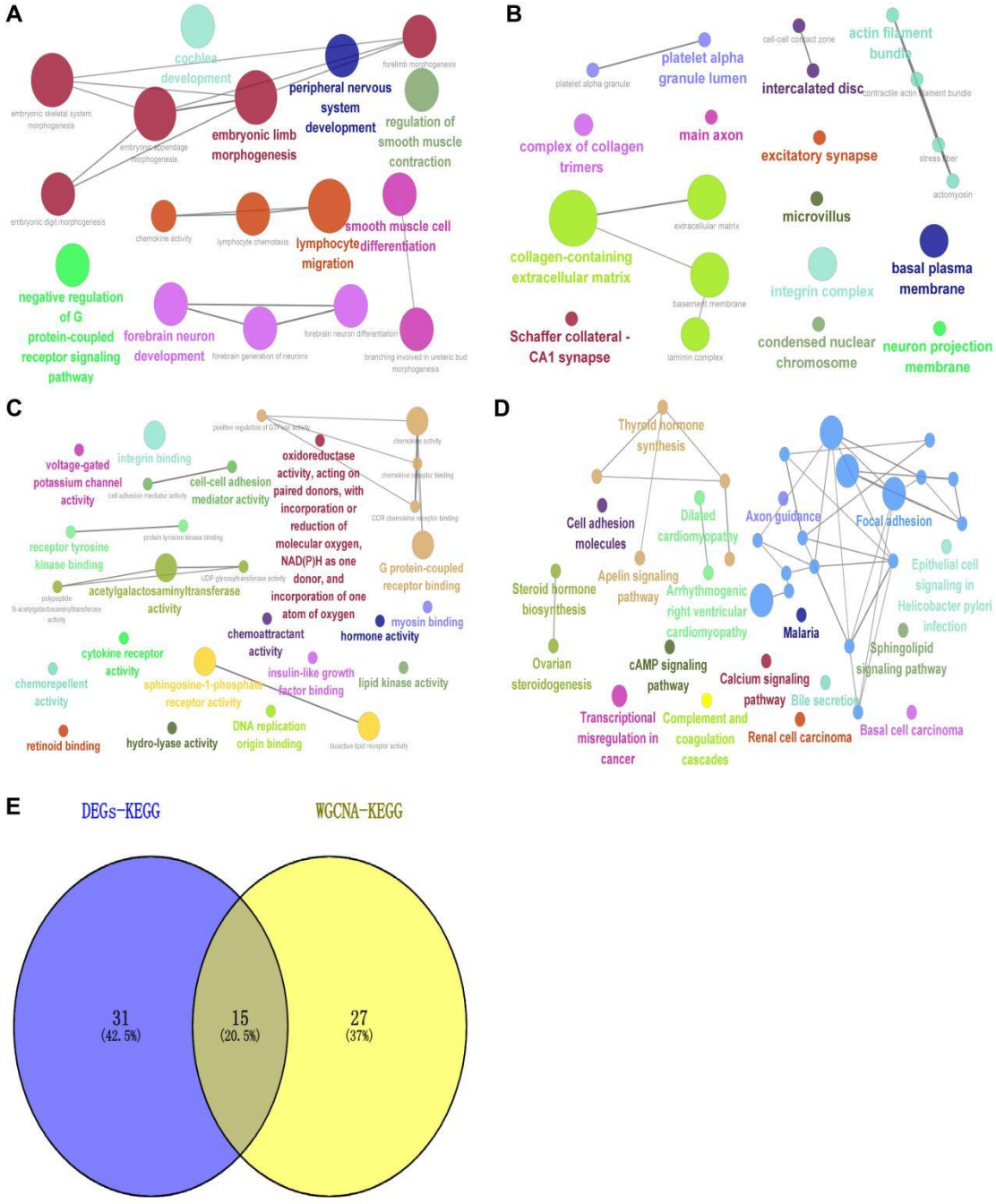


Figure 5. Enrichment analysis of lipoma pathologic characteristic genes. (A) BP display. (B) CC display. (C) MF display. (D) KEGG display. (E) DEG-KEGG and WGCNA-KEGG Venn diagrams. BP, biological process; CC, cellular component; MF, molecular function; KEGG, Kyoto Encyclopedia of Genes and Genomes.

GSEA enrichment analysis validation

To further validate the 15 obtained signalling pathways associated with lipomas, we performed GSEA enrichment analysis on the entire dataset. BP (Figure 6A) enrichment included NEGATIVE_REGULATION_OF_CATION_TRANSMEMBRANE_TRANSPORT. CC (Figure 6B) enrichment included CELL_DIVISION_SITE. MF (Figure 6C) enrichment included GROWTH_FACTOR_BINDING. KEGG (Figure 6D) pathway enrichment included the calcium signalling pathway and STEROID_HORMONE_BIOSYNTHESIS. These results validated 9 signalling pathways associated with lipoma.

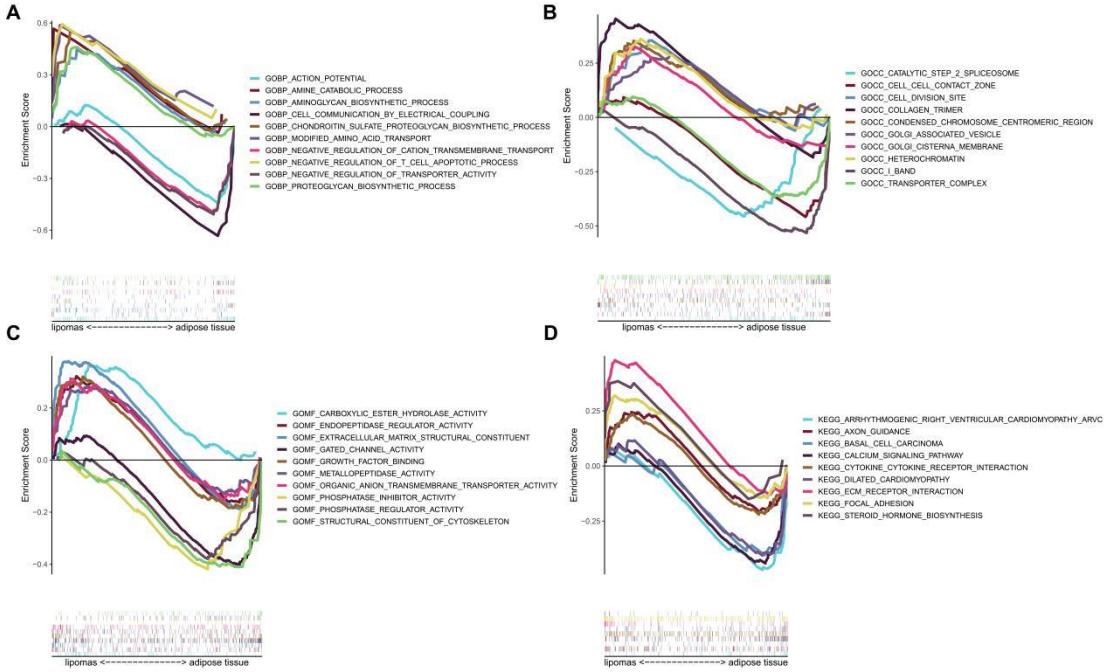


Figure 6. GSEA enrichment validation analysis. (A) BP display. (B) CC display. (C) MF display. (D) KEGG display. BP, biological process; CC, cellular component; MF, molecular function; KEGG, Kyoto Encyclopedia of Genes and Genomes.

Discussion

Lipomas arise in the body with accumulation of fat. Superficial fat accumulation can cause changes in body shape, but some deeper lipomas have proven complications, particularly intraosseous lipomas(24). To date, frontal bone lipomas (25), cranial bone lipomas (26), carpal bone lipomas (27), intrapalpebral lipomas (28), and heel bone lipomas (29), among others, which are very difficult to remove surgically, have been reported. However, most of the literature on lipomas involves medical history reports, and the key genes and signalling pathways involved in lipoma development are not well understood. In this study, we used a bioinformatic approach to identify hub genes and key signalling pathways in the development of lipomas, providing new insights into their early diagnosis and targeted treatment.

We first retrieved GSE141027 raw data from the GEO database for lipoma phenotype sequencing, synthesized the individual sample files into one expression profile file, used the edgeR package of R software to perform differential analysis on the expression profile files, and found 418 DEGs according to the filtering criteria, of which 176 were upregulated and 242 downregulated. Then, the MCODE plugin was used to analyse 5 key modules (with a score greater than 3) for a total of 59 key genes, and then the Hubba plugin was used to analyse central genes. The top 20 were selected as key genes, and the top 20 genes with the highest number of nodes were selected according to the neighbouring node algorithm (CKM, ATP2A1, MYLPF, TNNI2, MYL1, ACTN3, ACTN2, ACTG2, MYH11, NEB, MYBPC2, MYOZ1, MYH2, MYBPC1, TNNC2, ACTA1 and TCAP). CKM has been reported to be a biomarker for upregulation of muscle genes after exercise and is likely to affect fat consumption after exercise (30). Mylpf is a structural gene for muscle expressed in adipocytes (31). Loss of ACTN3 leads to superior resistance to cold and muscle heat production (32). ACTN2 expression is upregulated 3.3-fold during myogenic differentiation of skeletal muscle (33). Myh11 is involved in differentiation of adipose stem cells (34). MYH2 is significantly differentially expressed in adipose tissue (35). These genes are likely to be important for adipose tumours, ATP2A1, TNNI2, MYL1, and ACTG2, NEB, MYBPC2, MYOZ1, MYBPC1, TNNC2 and TCAP need to be further explored.

Enrichment analysis of DEGs was then performed to identify functional and signalling pathways, revealing 49 enriched pathways. Twenty-seven modules in the dataset were then analysed using WGCNA for their relevance to the clinicopathological features of lipoma, with the highest correlation index of positive and negative correlation selected as the key modules. The intersection of 42 signalling pathways was used to obtain 15 important signalling pathways (Table 1), and then the whole sample was validated using GSEA. Of these, the P values for the calcium signalling pathway, ECM-receptor interaction and arrhythmogenic right ventricular

cardiomyopathy were less than 0.05, which was statistically significant. The calcium signalling pathway (36) is extensively involved in regulation of adipose differentiation (37), and the ECM-receptor interaction is likely to play a role in regulation of adipose differentiation, with an important function in adipose differentiation (38). These signalling pathways may be closely related to the development of lipomas, and other signalling pathways need to be further explored.

Table 1. Table of signalling pathways

Serial number	Signalling pathway name
1	Steroid hormone biosynthesis
2	AGE-RAGE signalling pathway in diabetic complications
3	Axon guidance
4	Apelin signalling pathway
5	Cell adhesion molecules
6	Calcium signalling pathway
7	Malaria
8	Cytokine–cytokine receptor interaction
9	Viral protein interaction with cytokine and cytokine receptor
10	Focal adhesion
11	ECM-receptor interaction
12	Arrhythmogenic right ventricular cardiomyopathy
13	Dilated cardiomyopathy
14	Basal cell carcinoma
15	Gastric cancer

Our study has some limitations. First, the key genes and signalling pathways we analysed were not experimentally validated. Second, the sample size of each group was not large, and further studies are needed.

Conclusions

In this study, we identified 17 hub genes associated with the development of lipomas and 9 important signalling pathways, and 3 were statistically significant in GSEA enrichment analysis. These findings provide new insights into the underlying molecular mechanisms of lipoma development and progression.

ABBREVIATIONS: GEO, Gene Expression Omnibus; WGCNA, Weighted Gene coexpression Network Analysis; BP, biological process; CC, cellular component; MF, molecular function; KEGG, Kyoto Encyclopedia of Genes and Genomes; PPI, protein–protein interaction; TOM, topological overlap matrix; DEGs, differentially expressed genes, GO, Gene Ontology; GSEA, Genome enrichment analysis; MsigDB, Molecular Signature Database; NES, Normalized Enrichment Score; Log2FC, Log 2 Fold Change

ACKNOWLEDGEMENTS: Not applicable.

Ethics approval and consent to participate: Not applicable.

Consent for publication: Not applicable.

ADDITIONAL INFORMATION AND DECLARATIONS

Data availability declarations: The datasets presented in this study can be found in the following repositories: https://www.ncbi.nlm.nih.gov/geo/ and https://string-db.org/.

Author contributions: Fei Wang and Yuyang Xia: design and initiation of the study, monitoring of data quality, data analysis and interpretation, manuscript preparation and editing and acquisition of data. Yating Zhang: experimental operation and data acquisition. Yuxin Jia,Zhuyuan Zhang,Yu Deng and Yujing Wu: research concept and design and initiation. The final version of the manuscript was reviewed and approved by all authors.

Conflict of interest: The authors claim that the study was conducted without any commercial or financial relationship, which could be interpreted as a potential conflict of interest.

Funding: The present study was supported by the National Natural Science Foundation of China (Grant No. 81772383) and the Funded by Outstanding Leaders Training Program of Pudong Health Bureau of Shanghai (Grant No. PWRL2019-01) and the Funded by Shanghai Pudong Gongli Hospital Youth

Foundation (Grant No. 2022YQNJJ-09).

References

1. Bharti SK, Shannon BA, Sharma RK, Levin AS, Morris CD, Bhujwalla ZM, Fayad LM. 2022. Characterization of lipomatous tumors with high-resolution (1)H MRS at 17.6T: Do benign lipomas, atypical lipomatous tumors and liposarcomas have a distinct metabolic signature? Front Oncol 12:920560.
2. Bardazzi F, Starace M, Loi C, Filippi F, Peron I, Sacchelli L. 2024. More than mere lipomas? J Dtsch Dermatol Ges 22:601-603.
3. Goto T, Kogure A, Kuwano Y. 2022. Lipomas at the site of chronic compression. Int J Dermatol 61:e328-e329.
4. Dupuis H, Lemaitre M, Jannin A, Douillard C, Espiard S, Vantyghem MC. 2024. Lipomatoses. Ann Endocrinol (Paris) 85:231-247.
5. Ben Ali H, Batarfi L, Aldraihem MO, Bashir S. 2022. Unusual presentation of a giant thoracic spinal cord lipoma. Spinal Cord Ser Cases 8:35.
6. Dusseau NB, 2nd, Khalafallah AM, Xu KY, Burks SS, Levi AD. 2025. Brachial Plexus Lipoma Causing Neurological Impairment: A Case Series and Systematic Review. Neurosurgery doi:10.1227/neu.0000000000003432.
7. Klubíčková N, Billings S, Dermawan JKT, Molligan JF, Fritchie K. 2025. Ossifying fibromyxoid tumours with lipomatous and cartilaginous differentiation: A diagnostic pitfall. Histopathology 86:891-899.
8. Xu S, Li X, Zhang S, Qi C, Zhang Z, Ma R, Xiang L, Chen L, Zhu Y, Tang C, Bourgonje AR, Li M, He Y, Zeng Z, Hu S, Feng R, Chen M. 2023. Oxidative stress gene expression, DNA methylation, and gut microbiota interaction trigger Crohn's disease: a multi-omics Mendelian randomization study. BMC Med 21:179.
9. Sun HW, Zhang X, Shen CC. 2024. The shared circulating diagnostic biomarkers and molecular mechanisms of systemic lupus erythematosus and inflammatory bowel disease. Front Immunol 15:1354348.
10. Rather MA, Agarwal D, Bhat TA, Khan IA, Zafar I, Kumar S, Amin A, Sundaray JK, Qadri T. 2023. Bioinformatics approaches and big data analytics opportunities in improving fisheries and aquaculture. Int J Biol Macromol 233:123549.
11. Daou R, Beißbarth T, Wingender E, Gültas M, Haubrock M. 2020. Constructing temporal regulatory cascades in the context of development and cell differentiation. PLoS One 15:e0231326.
12. Nawaz MA, Pamirsky IE, Golokhvast KS. 2024. Bioinformatics in Russia: history and present-day landscape. Brief Bioinform 25.
13. Chen G, Gou B, Du Y, Zhou Z, Bai Y, Yang Y, Nan Y, Yuan L. 2025. Predicting the molecular mechanism of ginger targeting PRMT1/BTG2 axis to inhibit gastric cancer based on WGCNA and machine algorithms. Phytomedicine 143:156892.
14. Xu M, Zhou H, Hu P, Pan Y, Wang S, Liu L, Liu X. 2023. Identification and validation of immune and oxidative stress-related diagnostic markers for diabetic nephropathy by WGCNA and machine learning. Front Immunol 14:1084531.
15. Zhu X, Yin T, Zhang T, Zhu Q, Lu X, Wang L, Liao S, Yao W, Zhou Y, Zhang H, Li X. 2022. Identification of Immune-Related Genes in Patients with Acute Myocardial Infarction Using Machine Learning Methods. J Inflamm Res 15:3305-3321.
16. Feng S, Xu Y, Dai Z, Yin H, Zhang K, Shen Y. 2022. Integrative Analysis From Multicenter Studies Identifies a WGCNA-Derived Cancer-Associated Fibroblast Signature for Ovarian Cancer. Front Immunol 13:951582.
17. Wang Z, Hu D, Pei G, Zeng R, Yao Y. 2023. Identification of driver genes in lupus nephritis based on comprehensive bioinformatics and machine learning. Front Immunol 14:1288699.
18. Wang H, Zhang Z, Ma Y, Jia Y, Ma B, Gu J, Chen O, Yue S. 2022. Construction of Severe Eosinophilic Asthma Related Competing Endogenous RNA Network by Weighted Gene Co-Expression Network Analysis. Front Pharmacol 13:852536.
19. Harutyunyan A, Chong D, Li R, Shah AD, Ali Z, Huang C, Barlow CK, Perucca P, O'Brien TJ, Jones NC, Schittenhelm RB, Anderson A, Casillas-Espinosa PM. 2022. An Integrated Multi-Omic Network Analysis Identifies Seizure-Associated Dysregulated Pathways in the GAERS Model of Absence Epilepsy. Int J Mol Sci 23.
20. Chen Y, Chen L, Lun ATL, Baldoni PL, Smyth GK. 2025. edgeR v4: powerful differential analysis of

sequencing data with expanded functionality and improved support for small counts and larger datasets. Nucleic Acids Res 53.

21. Szklarczyk D, Gable AL, Nastou KC, Lyon D, Kirsch R, Pyysalo S, Doncheva NT, Legeay M, Fang T, Bork P, Jensen LJ, von Mering C. 2021. The STRING database in 2021: customizable protein-protein networks, and functional characterization of user-uploaded gene/measurement sets. Nucleic Acids Res 49:D605-d612.
22. Xiong Y, Liu X, Jiang L, Hao T, Wang Y, Li T. 2024. Inhibition of ferroptosis reverses heart failure with preserved ejection fraction in mice. J Transl Med 22:199.
23. Ono K, Fong D, Gao C, Churas C, Pillich R, Lenkiewicz J, Pratt D, Pico AR, Hanspers K, Xin Y, Morris J, Kucera M, Franz M, Lopes C, Bader G, Ideker T, Chen J. 2025. Cytoscape Web: bringing network biology to the browser. Nucleic Acids Res doi:10.1093/nar/gkaf365.
24. Gitto S, Doeleman T, van de Sande MAJ, van Langevelde K. 2022. Intraosseous hibernoma of the appendicular skeleton. Skeletal Radiol 51:1325-1330.
25. Schmidt J, Bremmer F, Brockmann K, Kaulfuß S, Wollnik B. 2022. Progressive frontal intraosseous lipoma: Detection of the mosaic AKT1 variant discloses Proteus syndrome. Clin Genet 102:239-241.
26. Nagase S, Ogura K, Ashizawa K, Sakaguchi A, Hotchi S, Hishii M, Fukunaga M, Matsumoto T. 2022. Intraosseous Lipoma of the Calvaria in the Early Stage Resembling Normal Fatty Marrow. J Neurol Surg Rep 83:e29-e32.
27. Park IJ, Lee J, Lee H, Kang SH. 2022. Intraosseous Lipoma of the Carpus: A Report of 2 Cases and a Review of the Literature. Ann Plast Surg 89:286-291.
28. Khanduri S, Malik S, Khan N, Kaushik S, Panwar M. 2022. Sphenoclival Intraosseous Lipoma: A Typical Lesion at an Atypical Location. Cureus 14:e21732.
29. Toepfer A, Strässle M, Lenze U, Lenze F, Harrasser N. 2023. Allogenic Cancellous Bone versus Injectable Bone Substitute for Endoscopic Treatment of Simple Bone Cyst and Intraosseous Lipoma of the Calcaneus and Is Intraosseous Lipoma a Developmental Stage of a Simple Bone Cyst? J Clin Med 12.
30. Ndumele CE, Neeland IJ, Tuttle KR, Chow SL, Mathew RO, Khan SS, Coresh J, Baker-Smith CM, Carnethon MR, Després JP, Ho JE, Joseph JJ, Kernan WN, Khera A, Kosiborod MN, Lekavich CL, Lewis EF, Lo KB, Ozkan B, Palaniappan LP, Patel SS, Pencina MJ, Powell-Wiley TM, Sperling LS, Virani SS, Wright JT, Rajgopal Singh R, Elkind MSV, Rangaswami J. 2023. A Synopsis of the Evidence for the Science and Clinical Management of Cardiovascular-Kidney-Metabolic (CKM) Syndrome: A Scientific Statement From the American Heart Association. Circulation 148:1636-1664.
31. Huang C, Zhang D, Wang Z, Zhao Y, Blecker C, Li S, Zheng X, Chen L. 2023. Validation of protein biological markers of lamb meat quality characteristics based on the different muscle types. Food Chem 427:136739.
32. Zouhal H, Coso JD, Jayavel A, Tourny C, Ravé G, Jebabli N, Clark CCT, Barthélémy B, Hackney AC, Abderrahman AB. 2023. Association between ACTN3 R577X genotype and risk of non-contact injury in trained athletes: A systematic review. J Sport Health Sci 12:359-368.
33. Walsh R, Offerhaus JA, Tadros R, Bezzina CR. 2022. Minor hypertrophic cardiomyopathy genes, major insights into the genetics of cardiomyopathies. Nat Rev Cardiol 19:151-167.
34. Biswas L, Chen J, De Angelis J, Singh A, Owen-Woods C, Ding Z, Pujol JM, Kumar N, Zeng F, Ramasamy SK, Kusumbe AP. 2023. Lymphatic vessels in bone support regeneration after injury. Cell 186:382-397.e24.
35. Bataille S, McKay N, Koppe L, Beau A, Benoit B, Bartoli M, Da Silva N, Poitevin S, Aniort J, Chermiti R, Burtey S, Dou L. 2023. Indoxyl sulfate inhibits muscle cell differentiation via Myf6/MRF4 and MYH2 downregulation. Nephrol Dial Transplant 39:103-113.
36. Shao M, Teng X, Guo X, Zhang H, Huang Y, Cui J, Si X, Ding L, Wang X, Li X, Shi J, Zhang M, Kong D, Gu T, Hu Y, Qian P, Huang H. 2022. Inhibition of Calcium Signaling Prevents Exhaustion and Enhances Anti-Leukemia Efficacy of CAR-T Cells via SOCE-Calcineurin-NFAT and Glycolysis Pathways. Adv Sci (Weinh) 9:e2103508.
37. Nosrati H, Fallah Tafti M, Aghamollaei H, Bonakdar S, Moosazadeh Moghaddam M. 2024. Directed Differentiation of Adipose-Derived Stem Cells Using Imprinted Cell-Like Topographies as a Growth Factor-Free Approach. Stem Cell Rev Rep 20:1752-1781.

38. Chen C, Chen J, Wang Y, Fang L, Guo C, Sang T, Peng H, Zhao Q, Chen S, Lin X, Wang X. 2023. Ganoderma lucidum polysaccharide inhibits HSC activation and liver fibrosis via targeting inflammation, apoptosis, cell cycle, and ECM-receptor interaction mediated by TGF-β/Smad signaling. Phytomedicine 110:154626.